IOP Conf. Series: Journal of Physics: Conf. Series **1063** (2018) 012131 doi:10.1088/1742-6596/1063/1/012131

Crystal plasticity finite-element analysis of surface roughening behaviour in biaxial stretching of steel sheets

M. Kubo[1, 2], T. Hama[2], Y. Tsunemi[3], Y. Nakazawa[3], H. Takuda[2]

[1] Research & Development Bureau, Nippon Steel & Sumitomo Metal Corporation, Amagasaki, Hyogo, 660-0891, Japan
[2] Graduate School of Energy Science, Kyoto University, Kyoto 606-8501, Japan
[3] Research & Development Bureau, Nippon Steel & Sumitomo Metal Corporation, Futtsu, Chiba, 293-8511, Japan

E-mail: kubo.m9p.masahiro@jp.nssmc.com

Abstract. Because of the increasing demand for automobile outer panels with sharper streamlines, prevention of surface roughening during press forming is important to obtain outer panels with better surfaces. It is crucial to examine the effects of deformation-mode on surface roughening, because steel sheets are subjected to various deformation modes during press forming. Moreover, surface roughening behaviour of interstitial free (IF) steels, which are now commonly utilized for fabricating outer panels, has not been studied enough. In this study, surface roughening behaviours of IF steel under various deformation modes were simulated by crystal plasticity finite-element analysis (CPFEA). First, the validation of a CPFEA model was carried out for investigating the stress-strain relationships in simple shear deformation and for studying changes in crystal orientations during biaxial tension. Then, the influence of microstructures on surface roughening was investigated. The results showed that surface roughening was larger for plane-strain tension than for equi-biaxial tension in IF steels. To predict surface roughening, it is essential to consider the difference of deformation resistance between crystals and the distribution of crystal orientations in the thickness direction.

1. Introduction

Recently, exterior designs of automobiles have tended to become more complicated to meet the diverse needs of consumers. In draw and stretch forming of such panels, tools with small radii are usually used, which, however, can result into the so-called "surface roughness [1]" or "surface roughening". Therefore, it is desirable to reduce surface roughening as much as possible to improve the surface quality of the panels.

Studies to overcome surface roughening in press forming have been conducted for a long time. These studies, however, have been carried out mainly for aluminium alloy sheets (e.g. [2]); studies on steel sheets have been limited to common carbon steel sheets (e.g. [3]). For interstitial free (IF) steel sheets, which are now commonly utilized for outer panels, the knowledge about surface roughening, including the influence of microstructures on surface roughening, is lacking.

Surface roughening is affected by not only material factors [2, 3], such as crystal grain size and crystal microstructure, but also by forming conditions [1-3], such as the amount of strain and deformation mode, i.e. strain path. There are various deformation modes in biaxial stretching, for example, equi-biaxial tension and plane strain tension. As pointed out by Osakada et al. [3], the

behaviour of surface roughening is also affected by the deformation mode, and it is necessary to predict surface roughening with high precision for various deformation modes in order to improve the surface qualities.

Therefore, in the present study, the influence of the deformation mode on the surface roughness development of IF steels was numerically examined using crystal plasticity finite-element analysis (CPFEA) [4-6]. The differences in surface roughening behaviours and changes in the microstructure between the deformation modes were examined and compared with experimental results. The appropriate numerical modelling for surface roughening was also discussed.

2. Crystal Plasticity Finite-element method

2.1. CPFEA model used in this study

The influence of deformation mode on the surface roughening of a steel sheet was numerically analysed by CPFEA, because the difference in deformation resistance among crystal grains affects surface roughening [7]. CPFEA can simulate the evolution of crystal orientation and work hardening behaviour due to deformation. A strain-rate dependent model for bcc metals was utilized to represent the slip rate of each slip system [6]. Two families of slip systems, 12 {110} <111> and 12 {112} <111> slip systems, were considered [5]. The slip rate of each slip system $\dot{\gamma}^{\alpha}$ can be obtained by the following equation [4],

$$\dot{\gamma}^{\alpha} = \dot{\gamma}_0 \left(\frac{\tau^{\alpha}}{g^{\alpha}} \right)^{\frac{1}{m}} sign\left(\tau^{\alpha}\right) \tag{1}$$

where $\dot{\gamma}_0$ (0.002 /s) is the reference-strain rate and m (0.02) is the rate-sensitivity exponent; τ^{α} is the resolved shear stress acting on slip system α and g^{α} is the strength of each slip system, which corresponds to the critical resolved shear stress initially, and its evolution can be given as follows [5]:

$$\dot{g}^{\alpha} = \sum_{\beta}^{N} h_{\alpha\beta} \left| \dot{\gamma}^{\beta} \right| \tag{2}$$

$$h_{\alpha\beta} = q_{\alpha\beta} \left(C_1 g_1 e^{-C_1 \bar{\gamma}} + C_2 g_2 e^{-C_2 \bar{\gamma}} \right) \tag{3}$$

where N is the number of slip systems, and $q_{\alpha\beta}$ is the interaction matrix. All components in the interaction matrix are set to 1.0, following the literature [5]. C_1, C_2, g_1, and g_2 in equation (3) are material parameters; $\bar{\gamma}$ is the cumulative shear strain on all slip systems. The materials were prepared using the methods reported in literature, and the hardening parameters determined by Uenishi et al. [5] were employed (C_1 = 6.3, C_2 = 95.0, g_1 = 108 MPa, g_2 = 58 MPa).

Isotropic elasticity was assumed, and Young's modulus and Poisson's ratio were set to be 206 GPa and 0.3, respectively.

2.2. CPFEA model for simple shear deformation of single crystal

In order to examine the difference in deformation resistance depending on crystal orientations, the stress-strain relationship under simple shear of single crystals was simulated.

Table 1 presents the crystallographic orientations of the samples used in the present study. Three samples with different crystallographic orientations were employed. These crystal orientations were measured on the actual materials. The representative volume element was an eight-node solid element with selective reduced integration, and is shown in Figure 1. The same crystallographic orientation was embedded into all eight integration points. The plane y = 0 was fixed in the x, y and z directions, respectively. Displacement increments were given in the x direction on the plane y = 10.

Table 1. Euler angles (Bunge's law) of single crystal specimens

Orientation No.	$\phi 1$ (°)	Φ (°)	$\phi 2$ (°)
1	211.4	88.6°	164.9°
2	106.3	100.4°	64.7°
3	45.4	87.3°	254.9°

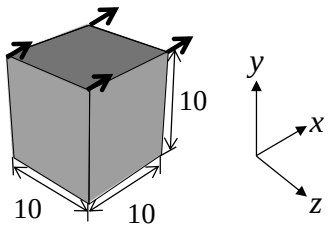

Figure 1. Numerical model for simple shear test.

2.3. CPFEA model for biaxial tension of poly-crystalline materials

Biaxial tension of a steel sheet was simulated to examine changes in the crystal orientations during deformation. The simulation result was also compared with the experimental result. In addition, the influence of the distribution of crystal orientations on surface roughening was investigated by the following two CPFEA models.

The first model is shown in Figure 2. This model was used to examine the effects of distribution of crystal orientations in the RD(rolling direction)-TD(transverse direction) plane on surface roughening. 200 μm^2 IPF maps of the RD-TD cross-section of samples were modelled by using 10,000 eight-node solid elements of length 2 μm, assuming columnar grains with a length of 2 μm in the depth direction. Displacement increments in the *x* direction were assigned to the front *y*-*z* plane, while the hidden *y*-*z* plane was fixed in the *x* direction. Displacement increments in the *y* direction were applied to the right *x*-*z* plane, while the left *x*-*z* plane was fixed in the *y* direction. Displacement boundary conditions were assigned to the sides of the square such that the equibiaxial tension or plane strain tension was realized. The bottom *x*-*y* plane was fixed in the *z* direction.

The second model is shown in Figure 3. This model was used to examine the effects of distribution of crystal orientations in the ND(normal direction)-RD plane. IPF maps of the ND-RD cross-section (150 μm in the longitudinal (x: RD) direction and 46 μm in the width (z: ND) direction) were modelled by using 5,000 eight-node solid elements with a length of 2 μm, assuming columnar grains with a length of 6 μm in the transverse direction. The crystal orientation distribution of the model was obtained by directly discretizing an IPF map in the RD-ND cross section of steel sheet. Displacement increments in the *x* direction were assigned to the right *y*-*z* plane, while the left *y*-*z* plane was fixed in the *x* direction. Displacement increments in the *y* direction were applied to the hidden *x*-*z* plane, while the front *x*-*z* plane was fixed in the *y* direction. The amounts of displacement in the *x* and *y* directions were set to follow the prescribed deformation mode. The bottom *x*-*y* plane was fixed in the *z* direction. The surface roughening can be determined from the profile of the upper free surface.

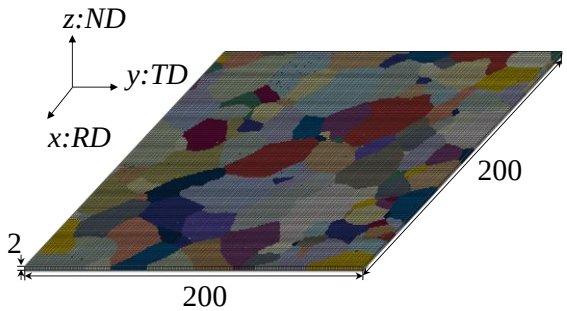

Figure 2. Numerical model of RD-TD plane of steel sheet for stretch forming.

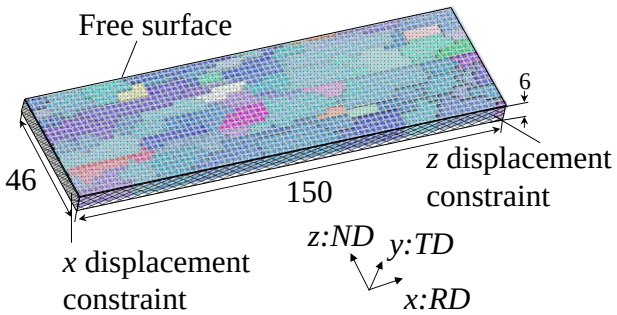

Figure 3. Numerical model of ND-RD plane of steel sheet for stretch forming.

3. Experimental procedures

3.1. Measurement of stress-strain relationships in simple shear deformation

Following the experiment conducted by Uenishi et al., the deformation behaviours in bcc single crystals with different crystallographic orientations, as shown Table 1, were employed for the simple shear test. For the preparation of the single crystal sheets and the experimental procedure of the simple shear test, please refer to the literature [5].

3.2. Measurement of development in surface roughening of steel sheet surface

The materials used in the present study were cold-rolled and annealed steel sheets comprising a single phase of ferrite. The mechanical properties of the materials are shown in Table 2. The materials comprised IF steel sheets; their microstructures are shown in Figure 4. The average grain sizes, *d*, of materials A and B were 29 μm and 16 μm, respectively.

Table 2. Mechanical properties of sheet steel materials.

Material	Initial Thickness (mm)	Yield Strength (MPa)	Tensile Strength (MPa)	Uniform Elongation[a] (%)	r-value[b]			Average *r*-value
					r_0	r_{45}	r_{90}	
IF steel A	1.60	150	287	29	1.7	1.5	2.1	1.7
IF steel B	0.75	185	340	25	1.2	1.8	1.7	1.6

[a] Measured in rolling (0°) direction.
[b] Measured at plastic strain of 0.15 in 0°, 45°, and 90° from the rolling direction

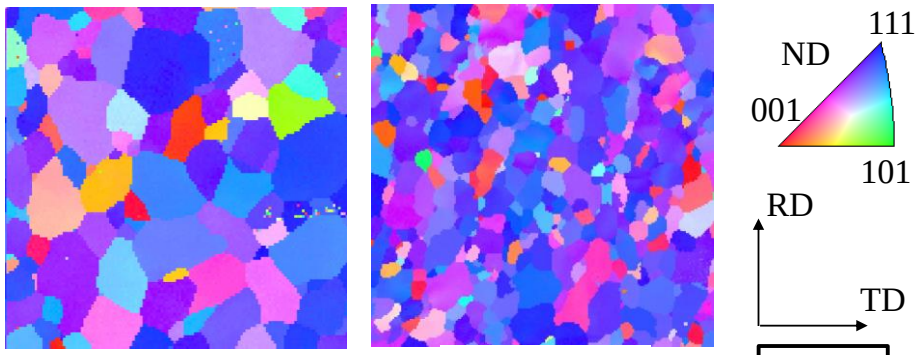

(a) IF steel A (d = 29 μm) (b) IF steel B (d = 16 μm)

Figure 4. Initial microstructure (IPF map) of materials at 0.1 mm from surface (*d*: average grain size).

To examine the difference in the surface roughening behaviour depending on the deformation mode, the change in the sheet surface in Marciniak type biaxial tension test [8] was first investigated. For the detailed experimental procedure, please refer to the literature [7]. Surface profiles after the test were measured using a contact-type roughness meter. Scanning was conducted in RD with a speed of 0.15 mm/s. In this paper, the arithmetical mean roughness profile, P_a [9], was used as a parameter that quantitatively represents the unevenness of the surface, because P_a could be easily obtained by numerical simulation.

Changes in the surface conditions, including the microstructure and profile, were observed continuously using a biaxial tension test system fitted inside a vacuum chamber of SEM (details of the experimental apparatus are given in our previous reports [7, 10]). Two types of deformation modes, equibiaxial tension and plane-strain tension, were employed by controlling the stroke motions in RD

and TD.in two directions. The equivalent plastic strain was evaluated from changes in distance between the crystal triple points in two directions.

4. Results and discussion

4.1. Stress-strain relationships in simple shear deformation

Figure 5 shows the comparison between CPFEA and experimental results of the shear stress-shear strain curves for the three crystal orientations. Although the stress values obtained by the simulation are somewhat larger than those obtained by the experiments, the simulation results agree qualitatively well with the experimental ones. Based on these results, it can be considered that the difference in deformation resistance depending on crystal orientations can be qualitatively reproduced by the CPFEA model used in the present study.

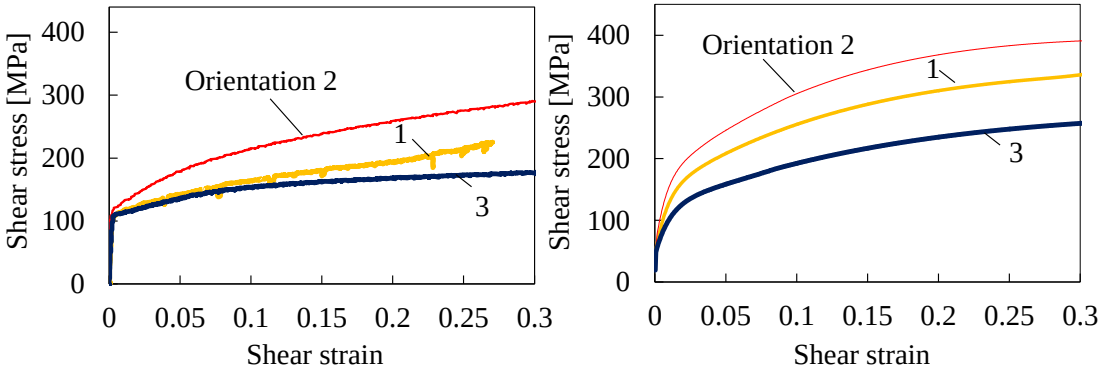

Figure 5. (a) Experimental and (b) numerical results of shear stress-shear strain curves obtained under simple shear of single crystals.

4.2. Changes of crystal orientations during biaxial tension

Figure 6 shows the comparison between CPFEA and experimental results of the changes in the crystal orientations of IF Steel A for equibiaxial tension. The model shown in Figure 2 was used. The IPF maps shown in the figure are the measured result before deformation. Changes in the orientations of grains 1, 2, and 3 until the strain of 0.13 for biaxial tension were measured and compared in the right figure. For all grains, the simulation results show good agreements with the experimental ones.

These results show that the CPFEA model used in this study is reliable for numerical simulations of surface roughening, where the stress and rotation of crystal grains play important roles.

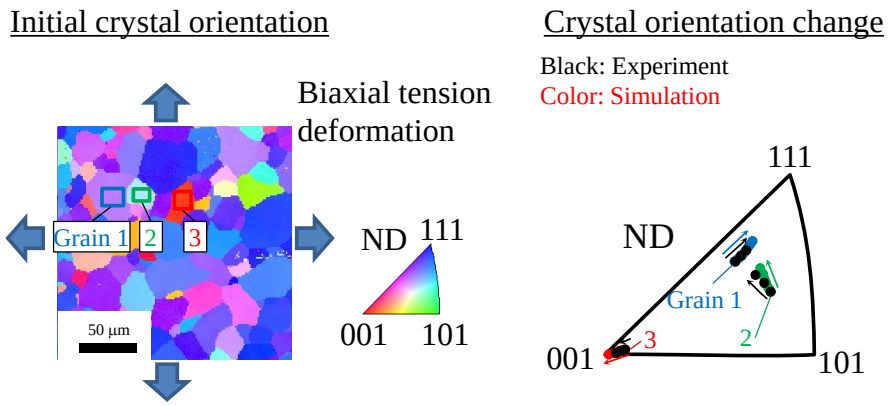

Figure 6. Variations in crystal orientation of IF steel A during equibiaxial tension.

4.3. Development in surface roughening

Figure 7 shows a comparison between the experimental and calculated changes of parameter P_a of IF Steel B during biaxial stretch forming. Because the surfaces of the real sheets in experiments were not perfectly flat before stretching, the comparison is carried out by increasing P_a from its initial value. The surface roughening of IF steel is comparatively large for plane strain tension in both the experiment and in CPFEA. The simulation results of the RD-TD model (figure 2) were much smaller than the experimental ones; parameter P_a was about 10 times smaller than the experimental result. However, the simulation results of the ND-RD model (figure 3) correspond well with the experimental ones, both qualitatively and quantitatively. These results suggest that to accurately evaluate the surface roughening, it is essential to consider not only the in-plane distribution of crystal orientations but also the distribution in the thickness direction.

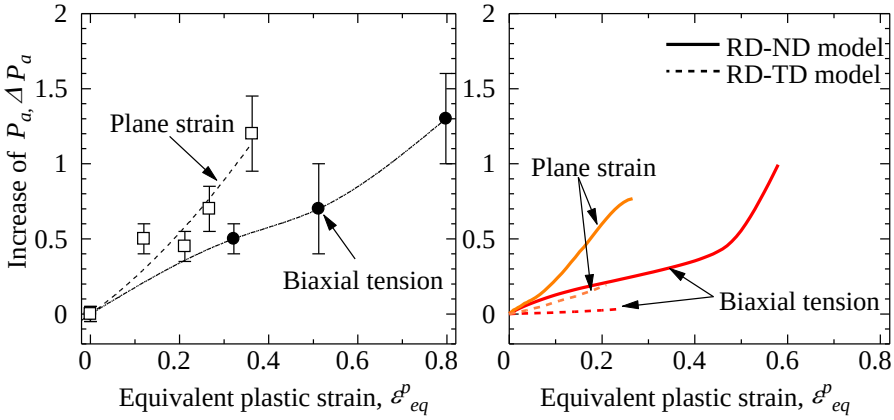

(a) Experiment (b) CPFEA

Figure 7. Comparison between (a) experimental and (b) CPFEA results of evolution of surface roughness for IF steel B.

5. Conclusions

The influence of the deformation mode on the surface roughness development of IF steels was numerically examined by CPFEA. The surface roughening of IF steel sheets is comparatively large for plane strain than for biaxial tension. The consideration of not only in-plane distribution of crystal orientations but also the distribution in the thickness direction is essential to evaluate surface roughening accurately.

References

[1] Kobayashi T, Murata K, Ishigaki H and Abe T 1970 *J. Jpn. Soc. Technol. Plasticity* **11** 495
[2] Becker R 1998 *Acta Mater.* **46** 1385
[3] Osakada K and Oyane M 1971 *Bull. JSME* **14** 171
[4] Asaro R J and Needleman A 1985 *Acta Metal.* **33** 923
[5] Uenishi A, Isogai E, Sugiura N, Ikematsu Y, Sugiyama M and Hiwatashi S 2013 *Nippon steel tech. rep.* **102** 57
[6] Hama T, Kojima K, Kubo M and Takuda H 2017 *ISIJ Int.* **57** 866
[7] Kubo M, Hama T, Tsunemi Y, Nakazawa Y and Takuda H 2018 *ISIJ Int.* **58** 704
[8] Marciniak Z and Kuczynski K 1967 *Int. J. Mech. Sci.* **9** 609
[9] ISO 3274: 1996. Geometrical Product Specifications (GPS)
[10] Kubo M, Yoshida H, Uenishi A, Suzuki S, Nakazawa Y, Hama T and Takuda H 2016 *ISIJ Int.* **56** 669